



ELSEVIER

Contents lists available at [ScienceDirect](http://www.sciencedirect.com)

Food and Bioproducts Processing

journal homepage: www.elsevier.com/locate/fbp

IChemE



The effect of gravity on moisture loss and oil absorption profiles during a simulated frying process using glass micromodels

Pablo Cortés^{a,b}, Luis Segura^c, Masahiro Kawaji^d, Pedro Bouchon^{a,b,*}

^a Department of Chemical and Bioprocess Engineering Pontificia Universidad, Católica de Chile P.O. Box 306, Santiago 6904411, Chile

^b ASIS-UC Interdisciplinary Research Program on Tasty and Healthy Foods, Pontificia Universidad Católica de Chile (PUC), Chile

^c Department of Food Engineering Universidad del Bío-Bío Avda. , Andrés Bello S/N, Chillán, Chile

^d Department of Mechanical Engineering, City College of New York, 160 Convent Ave., New York, 10031-9198, NY, United States of America

ARTICLE INFO

Article history:

Received 25 August 2014

Received in revised form 22 April 2015

Accepted 5 May 2015

Available online 14 May 2015

Keywords:

Micromodel

Frying

Oil uptake

Pore network

Capillaries

Dehydration

ABSTRACT

Great efforts have been made to elucidate the mechanisms responsible for oil absorption during deep-fat frying. This understanding can be certainly improved through direct visual observation. Accordingly, the goal of this study was to analyze mass transfer phenomena that develop during oil immersion by using glass micromodels partially submerged in oil (190 °C), to visualize the mechanisms responsible for moisture loss and oil absorption within a matrix, as well as the effect of gravity, for the first time, using three different configurations ($g = 0$, $g < 0$, and $g > 0$). Moisture and oil profiles were imaged during the frying process in order to obtain water and oil saturation maps. Drying and oil curves were constructed using image analysis, and fractal analysis was performed to describe the morphology of the evaporation and oil fronts. If $g < 0$ (open side of the micromodel at the bottom) drying times were shorter and gravity tended to destabilize the drying front, which had a mean fractal dimension of 1.818 ± 0.032 that was significantly higher ($p < 0.05$) than those obtained in other set-ups. Largely, evaporation fronts tended to take the form of temperature profiles as reflected by infrared thermal imaging. The morphology of the advancing oil fronts was similar in all configurations. However, g severely affected oil content. When $g = 0$, less oil was absorbed with a final oil saturation of 32%. In all configurations the air inlet was a key factor to stop oil suction. This occurred even though enough oil could still remain on the surface. Overall, these results may help scientists to describe the physical mechanisms that develop during oil immersion and help presenting an interesting approach that may be used in other fields. © 2015 The Institution of Chemical Engineers. Published by Elsevier B.V. All rights reserved.

1. Introduction

Over the past 20 years, several of the heat and mass transfer phenomena occurring during or immediately after deep frying have been described. Different contributions have

suggested that oil does not penetrate the food product while there is an overpressure inside (Dana and Saguy, 2006; Farinu and Baik, 2005; Mellema, 2003). Thus, oil absorption would be mostly absorbed during cooling, since the vigorous escape of water vapor would preclude oil absorption during most of the

* Corresponding author at: Department of Chemical and Bioprocess Engineering, Pontificia Universidad Católica de Chile, P.O. Box 306, Santiago 6904411, Chile. Tel.: +56 2 2354 4237; fax: +56 2 2354 5803.

E-mail address: pbouchon@ing.puc.cl (P. Bouchon).

<http://dx.doi.org/10.1016/j.fbp.2015.05.001>

0960-3085/© 2015 The Institution of Chemical Engineers. Published by Elsevier B.V. All rights reserved.

immersion period, as was indirectly determined by [Bouchon et al. \(2003\)](#). Accordingly, the pressure drop generated during cooling has been suggested as one of the main driving forces to control oil absorption ([Bouchon and Pyle, 2005a](#); [Mellema, 2003](#); [Ziaififar et al., 2008](#)), although some authors have mainly related it to capillary pressure ([Moreira and Barrufet, 1998](#)). [Bouchon and Pyle \(2005a\)](#) considered both effects, developing a modified form of the Washburn equation, which in addition to capillary pressure, included a new term that represented the unbalanced atmospheric pressure due to the change of the water vapor pressure during cooling, as well as the influence of gravity. However, models that have been developed are not accurate in predicting the time, quantity and location of the oil within the fried food, indicating that the phenomenon has not yet been fully understood.

So far, all of the models described have been developed from a macroscopic viewpoint and many authors have used diagrams with an ideal pore to explain the oil absorption phenomenon ([Mellema, 2003](#)). For instance, they neglect the interconnection between pores as well as the fact that pores may be filled or partly filled with water, air, vapor or oil, and that their evolution will depend on the condition of their neighboring pores. The evolution of pressure and temperature fields also influences whether the pores dry or fill with air, water or oil.

The pore network approaches have several advantages over the continuum approach (e.g., diffusion model) in which the microscopic complexities are lumped (e.g., effective diffusivities), which mostly are empirical constants ([Gueven and Hicsasmaz, 2013](#)). Experimentally, they include the use of micromodels, which are transparent networks of pores and constrictions that simulate the complexity of a porous media ([Oyarzún and Segura, 2009](#)). The applications of micromodels are varied ([Badillo et al., 2011](#); [Laurindo and Prat, 1998](#); [SanMartin et al., 2011](#); [Segura and Oyarzún, 2012](#); [Segura and Toledo, 2005a](#)) and are increasing, since they allow us to see the movement of the fluid interface and to distinguish between mechanisms that have similar behavior with respect to other phenomena.

[Lenormand et al. \(1988\)](#) conducted extensive work through pore network simulations and experiments with transparent

micromodels in order to show the different displacement drain type mechanisms (a wetting fluid displaces a non-wetting) of two immiscible fluids according to the capillary number (C) and the viscosity ratio (M). C is a dimensionless number that is a ratio between the viscous forces and capillary forces. In porous media for low capillary numbers, flow is dominated by capillary forces whereas for high capillary number the capillary forces are negligible compared to viscous ones, as shown in Eq. (1):

$$C = \frac{q\mu_w}{A\gamma \cos \phi} \quad (1)$$

where the numerator is the displacing fluid flow q (m^3/s) times the viscosity of the wetting fluid μ ($\text{kg}/(\text{m}\cdot\text{s})$) and the denominator is the flow cross-sectional area A (m^2) times the interfacial tension of the wetting fluid (γ in N/m) and the cos of contact angle ϕ (for water/glass ~ 0). M is the ratio between the viscosity of the non-wetting fluid (in the case of the immersion period, it is the vapor) and the viscosity of the wetting fluid (water), as defined in Eq. (2):

$$M = \frac{\mu_{nw}}{\mu_w} \quad (2)$$

[Lenormand and Zarcone \(1989\)](#) and [Lenormand et al. \(1988\)](#) developed a model that can reproduce flow transitions from capillary forces-dominated to viscous forces-dominated. These authors established the existence of a “phase diagram” for the displacement of two immiscible phases that is reproduced in [Fig. 1](#), based on the capillary number (C) and the viscosity ratio (M), which define the existing flow patterns and regions.

In addition, the flow in a porous medium may be affected by additional factors including the direction in which this flow occurs in relation to the force of gravity. [Laurindo and Prat \(1996\)](#) studied the effect of gravity on the drying front of a micromodel during isothermal drying. They considered three basic situations depending on the Bond number B , which is defined as:

$$B = \Delta\rho g a^2 \sin \theta / \gamma \quad (3)$$

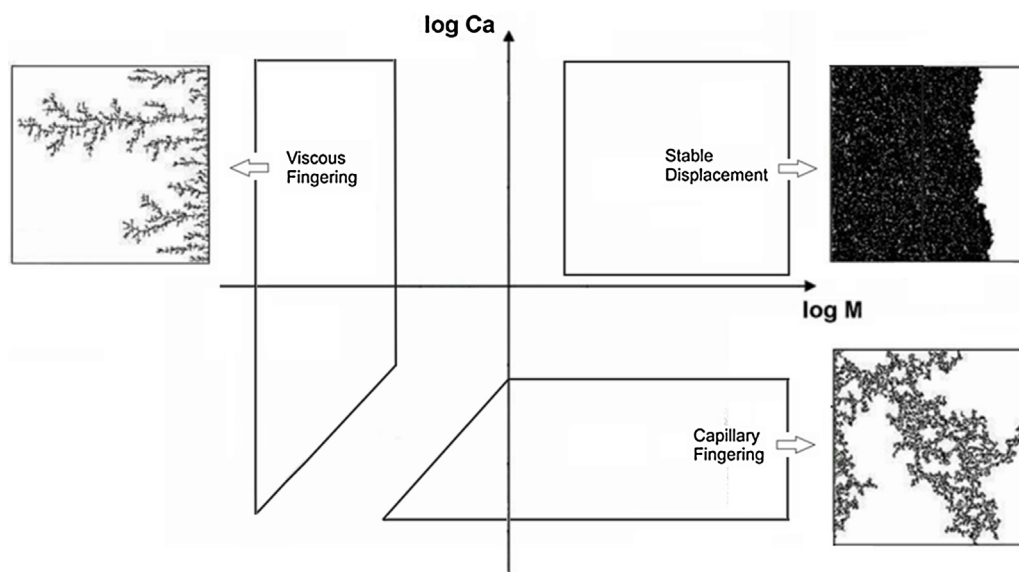


Fig. 1 – Phase diagram proposed by [Lenormand et al. \(1988\)](#) for drainage showing the different areas and types of profile found, adapted from [Badillo et al. \(2011\)](#).

Download English Version:

<https://daneshyari.com/en/article/19011>

Download Persian Version:

<https://daneshyari.com/article/19011>

[Daneshyari.com](https://daneshyari.com)